



HAL
open science

Acid-triggered Membrane Insertion of Pseudomonas Exotoxin A Involves an Original Mechanism Based on pH-regulated Tryptophan Exposure

Jocelyn Méré, Juliette Morlon-Guyot, Anne Bonhoure, Laurent Chiche, Bruno Beaumelle

► **To cite this version:**

Jocelyn Méré, Juliette Morlon-Guyot, Anne Bonhoure, Laurent Chiche, Bruno Beaumelle. Acid-triggered Membrane Insertion of Pseudomonas Exotoxin A Involves an Original Mechanism Based on pH-regulated Tryptophan Exposure. *Journal of Biological Chemistry*, 2005, 280 (22), pp.21194-21201. 10.1074/jbc.M412656200 . hal-02137183

HAL Id: hal-02137183

<https://hal.science/hal-02137183>

Submitted on 10 Nov 2020

HAL is a multi-disciplinary open access archive for the deposit and dissemination of scientific research documents, whether they are published or not. The documents may come from teaching and research institutions in France or abroad, or from public or private research centers.

L'archive ouverte pluridisciplinaire **HAL**, est destinée au dépôt et à la diffusion de documents scientifiques de niveau recherche, publiés ou non, émanant des établissements d'enseignement et de recherche français ou étrangers, des laboratoires publics ou privés.

Acid-triggered Membrane Insertion of *Pseudomonas* Exotoxin A Involves an Original Mechanism Based on pH-regulated Tryptophan Exposure*

Received for publication, November 9, 2004, and in revised form, March 29, 2005
Published, JBC Papers in Press, March 30, 2005, DOI 10.1074/jbc.M412656200

Jocelyn Méréz, Juliette Morlon-Guyot, Anne Bonhoure, Laurent Chiche, and Bruno Beaumelle

From the †Unite Mixte de Recherche 5539 CNRS, Case 107, Département Biologie-Santé, Université Montpellier II, 34095 Montpellier and §Centre de Biochimie Structurale, Unite Mixte de Recherche 5048 CNRS INSERM U554, Faculté de Pharmacie, 34093 Montpellier, France

Exposure to low endosomal pH during internalization of *Pseudomonas* exotoxin A (PE) triggers membrane insertion of its translocation domain. This process is a prerequisite for PE translocation to the cytosol where it inactivates protein synthesis. Although hydrophobic helices enable membrane insertion of related bacterial toxins such as diphtheria toxin, the PE translocation domain is devoid of hydrophobic stretches and the structural features triggering acid-induced membrane insertion of PE are not known. Here we have identified a molecular device that enables PE membrane insertion. This process is promoted by exposure of a key tryptophan residue. At neutral pH, this Trp is buried in a hydrophobic pocket closed by the smallest α -helix of the translocation domain. Upon acidification, protonation of the Asp that is the N-cap residue of the helix leads to its destabilization, enabling Trp side chain insertion into the endosome membrane. This tryptophan-based membrane insertion system is surprisingly similar to the membrane-anchoring mechanism of human anaxin-V and could be used by other proteins as well.

Exotoxin A (PE)¹ is one of the major virulence factors secreted by *Pseudomonas aeruginosa*. This toxin is able to kill a large range of mammalian cell lines by inhibiting their protein synthesis (1), and it is one of the favorite toxins to prepare immunotoxins that are promising agents for the treatment of cancers (2). PE is a single chain 66-kDa protein organized in three structural (3) and functional (4) domains successively involved in the intoxication process. First, domain I binds to the α_2 -macroglobulin/low density lipoprotein receptor-related protein (5), enabling internalization via receptor-mediated endocytosis. Domain II will then mediate translocation into the cytosol of the entire toxin (6) or of a carboxyl-terminal fragment generated by furin proteolysis and encompassing domain III and most of domain II (1). Finally, domain III will catalyze the ADP ribosylation of elongation factor 2, thereby inhibiting protein synthesis and killing the cell (1).

Several studies using model systems demonstrated the abil-

ity of PE to insert into membranes upon acidification (7, 8). Because cell intoxication by PE requires low endosomal pH (1, 6), it is also clear that this membrane insertion process is an essential step of the intoxication procedure. Nevertheless, the molecular bases for acid-triggered PE membrane insertion are not known. Indeed, although the translocation domains of related toxins such as diphtheria toxin or colicins show a characteristic three-layer structure with buried hydrophobic helices likely implicated in membrane insertion, PE domain II is devoid of such helices and, more generally, of hydrophobic stretches (9). This domain has no known homolog, and sequence (BLAST) (10) or structure (DALI) (11) searches yielded no significant hits. Moreover, no clear low pH sensor was found by examining the PE three-dimensional structure or using theoretical computations (12).

The PE translocation domain (domain II) that mediates translocation is small (102 residues) and constituted of six consecutive α -helices (A–F) (3). Most point mutations in domain II led to less toxic mutants (13, 14). These results indicated that most residues in the translocation domain are significantly involved in the overall toxicity of the molecule. Nevertheless, they did not allow identification of a critical portion of the domain implicated in membrane insertion and translocation.

More recently, our group sequentially deleted the six helices of domain II. Surprisingly, although deletion of any of the first five helices abrogates both translocation activity and toxicity, excising the smallest and last helix of the domain (helix F, 5 residues) increased the translocation rate by 60–70% with a concomitant ~4-fold rise in toxicity (15). This result indicated that this region has a key role in the translocation process.

In the present study, we looked for the molecular basis of the gain in translocation activity caused by helix F deletion. This work enabled us to identify the PE initial membrane insertion mechanism. Indeed, examination of the three-dimensional structure of PE (3) suggested that one main effect of helix F removal would be increased exposure of Trp-305 to the outside of the molecule. Here we have shown that this tryptophan is a key residue for PE acid-triggered membrane insertion and translocation. We also found that Asp-358, which is the helix F N-cap residue, is the low pH sensor triggering helix F destabilization leading to Trp-305 membrane insertion and toxin translocation at low pH.

MATERIALS AND METHODS

Structure Analyses and Modeling—The three-dimensional structure of PE at 3 Å resolution (3) was kindly provided by Dr. David McKay (Stanford, CA) and used for analysis and modeling. The refined structure published later (12) displays no significant differences in

* This work was supported by grants from the Association pour la Recherche sur le Cancer. The costs of publication of this article were defrayed in part by the payment of page charges. This article must therefore be hereby marked "advertisement" in accordance with 18 U.S.C. Section 1734 solely to indicate this fact.

† To whom correspondence should be addressed. Tel.: 33-467-14-33-98; Fax: 33-467-14-42-86; E-mail: beaume@univ-montp2.fr.

¹ The abbreviations used are: PE, *Pseudomonas* exotoxin A; PE-LL, PE large loop (PE-253C,364C); PE-SL, PE small loop (PE-304C,359C); SUV, small unilamellar vesicle; Mes, 4-morpholineethanesulfonic acid.

the structural regions discussed in this report and was only considered to check that no error was caused by the lower resolution of the structure used. The MODELLER program (16) was used to build models of the DelF mutant in which the EAGAANA sequence of the 359–365 segment was replaced by the Pro-Gly sequence (15) and of the PE-SL and PE-LL disulfide bonded mutants. The modeling was performed on the entire PE protein, including domains I and III, to check the possible impact of the modifications on interdomain contacts. Figures of structures were produced with the MOLMOL (17) and POV-Ray (www.povray.org) programs.

Materials—Chemicals were obtained from Sigma except for 1,2-dibromostearoyl-sn-glycero-3-phosphocholine, which was purchased from Avanti Polar Lipids. [³⁵S]Methionine (Trans-label) and ³²P-NAD were from MP Biomedicals.

Mutagenesis—pET-3d expression vector containing the PE coding sequence behind the pro-OmpA signal sequence was used as template for PCR-based mutagenesis (18). To construct PE-E359A, PE-E359P, PE-D358G, and PE-D358G,E359A, 5'-mutagenic primers in which GACGAG coding for Asp-358 and Glu-359 was, respectively, changed to GACGCG, GACCCG, GGCGAG, and GGCGCG were used together with a 3'-primer overlapping the PE-BamHI site to prepare a downstream PCR fragment. A 3'-mutagenic primer and a 5'-primer spanning the PE-NcoI site enabled us to obtain the upstream PCR fragment. These overlapping fragments were then joined and amplified by PCR using the outer primers. The resulting NcoI-BamHI fragment was inserted into pET3d-PE for expression. Trp-305 was changed into Ala or Phe by mutating its TGG codon to GCG or TTC, respectively. To obtain PE-S304C,E359C (PE-SL) and PE-G253C,N364C (PE-LL), three mutated fragments were produced and joined using the same strategy, changing the TCT and GAG codon of Ser-304 and Glu-359 to TGT and the GGC and AAC codons of Gly-253 and Asn-364 to TGC. All PCR-amplified DNA fragments were sequenced.

Protein Expression and Purification—*Escherichia coli* BL21 (ΔDE3) cells carrying the expression plasmid were grown at 37 °C in L-broth containing ampicillin (100 μg/ml). Isopropyl-β-D-thiogalactoside (1 mM) was added when A₆₀₀ reached 0.6; bacteria were harvested 2 h later. The periplasmic fraction prepared by osmotic shock was dialyzed against 20 mM Tris-HCl, pH 7.6 (buffer A), applied to a Q-Sepharose column, and eluted with a linear gradient (0–1 M) of NaCl in buffer A. If necessary, the protein was further applied to a Mono-P column (Amersham Biosciences) and eluted with a linear NaCl gradient (0–0.7 M in buffer A) (19). Toxin purity was verified on SDS-PAGE and was >90%.

Conformation Controls—We performed a number of control studies on the mutants. As shown earlier for deletion mutants (15), none of the mutations generated for this study in the translocation domain significantly affected the activity of the neighbor domains. This was checked by examining endocytosis and catalytic activity for domains I and III, respectively. We also verified using circular dichroism (15) and gel filtration experiments (19) that the mutations did not modify the overall structure of the molecule. Moreover, intracellular processing of PE by furin (15) was not affected by the mutations (data not shown). Altogether, these control experiments indicated that the mutations did not induce any long-distance modifications.

Preparation of Small Unilamellar Vesicles (SUVs)—Mixtures containing 75% 1,2-dioleoyl-sn-glycero-3-phosphocholine and 25% 1,2-diacyl-sn-glycero-3-phospho-(1-*rac*-glycerol) in CHCl₃ were dried under a stream of N₂ with a TurboVap LV evaporator (ZyMark). They were further desiccated under high vacuum for 1 h. The dried lipids were resuspended in 2 mM Tris, pH 7.0, at a final concentration of 10 mg/ml and then sonicated with a microtip sonicator (Branson digital sonifier) at 10% amplitude until optically clear. Brominated vesicles were prepared from mixtures containing 37.5% 1,2-dioleoyl-sn-glycero-3-phosphocholine, 25% 1,2-diacyl-sn-glycero-3-phospho-(1-*rac*-glycerol), and 37.5% 1,2-dibromostearoyl-sn-glycero-3-phosphocholine.

Fluorescence Spectroscopy—A PerkinElmer SS35 spectrofluorometer and semi-micro quartz 500-μl cuvettes were used. Slit widths were 2.5 nm for excitation and 2.5 nm for emission. Fluorescence intensity was measured at 350 nm using excitation at 280 nm. Buffer fluorescence was measured and subtracted. Experiments were performed using 10 μg/ml protein in 150 mM NaCl, 50 mM Mes at the indicated pH values. SUVs were used at a final concentration of 0.4 mg/ml. Quencher and SUV concentrations were high enough to produce minimal toxin dilution, which was taken into account for calculation (7).

Internalization and ADP Ribosylation Assays—Mutant internalization by mouse lymphocytes was assayed as described (6). The intracellular pathway of the mutants was studied by immunofluorescence (20). Upon endocytosis by L929 cells, PE and all mutants became concen-

trated with transferrin in the perinuclear recycling compartment (data not shown), as observed earlier in T-cells (6).

Endosome Fractionation and Cell-free Assay for PE Translocation—This assay has been described earlier (6, 15). Briefly, BW5147 mouse lymphocytes were labeled for 45 min with the ¹²⁵I-toxin. Endosomes were then purified using a discontinuous sucrose gradient, concentrated, and finally resuspended in translocation buffer containing 10 mM ATP/10 mM MgCl₂ and cytosol (~1 mg of protein/ml) (21). After 2 h at 37 °C, translocation was stopped by cooling on ice. Translocated toxin was then separated from endosomes by ultracentrifugation on a sucrose cushion. The supernatant/endosomes cpm ratio was plotted as a function of time. Translocation was linear with time over at least 2 h for all mutants, and the translocation rate was calculated using linear regression analysis (15).

Cytotoxicity Measurements—L929 cells were seeded into 96-well plates (7,000 cells/well) before adding the toxins. After 24 h at 37 °C, [³⁵S]methionine (500,000 cpm/well) was added, and cells were further incubated for 24 h before lysis in 0.1 M NaOH, collection of trichloroacetic acid-precipitable material by filtration, and scintillation counting. Control values and background incorporation were obtained in the absence of toxin and in the presence of 1 mM cycloheximide, respectively. The results are expressed as IC₅₀, which is the toxin concentration resulting in 50% protein synthesis inhibition.

Kinetics of Protein Synthesis Inhibition—To monitor the protein synthesis inactivation kinetics, L929 cells were treated with 10 μM toxin, and a 1-h pulse incorporation of [³⁵S]methionine in Dulbecco's modified Eagle's medium without methionine was performed at various times after the start of intoxication (20). Translocation activity was calculated as the inverse of t₅₀, which is the time required for 10 μM toxin to inhibit protein synthesis by 50%.

RESULTS

We examined the three-dimensional structure of the translocation domain (3) in an attempt to identify the structural basis of the gain in PE translocation activity obtained by deletion of helix F. This helix is extremely short (5 residues) and contains one Glu (Glu-359), three Ala, and one Gly. Glu-359 is hydrogen bonded with the backbone amide proton of Trp-305 (Fig. 1A), but other helix F residues did not appear to be critical for structural stability or interactions. Interestingly, Asp-358 is the N-cap residue of helix F (Fig. 1A) and, as such, likely plays a significant role in stabilizing the very short F α-helix. Molecular models of the DelF mutant were built using the MODELLER program (16) and confirmed that helix F removal was unlikely to significantly upset the structure. Structural modifications in all DelF models remained very limited (<0.5 Å) except in the immediate vicinity of the deletion. Accordingly, gel filtration experiments (19) and circular dichroism measurements (15) indicated that the PE structure is not significantly affected by excision of helix F.

The main finding from the comparison between wild-type PE and the DelF mutant was a clear increase, by about 25 Å² (Fig. 1B), in the solvent accessibility of the Trp-305 side chain in the DelF mutant and the opening of a possible channel that would allow Trp-305 to move toward the surface of the protein. Indeed, in PE, helix F partially masks the side chain of Trp-305, which is buried within a hydrophobic pocket (Fig. 1, A–C). The helix F deletion resulted in removal of the Glu-359-Trp-305 hydrogen bonding, but structural analysis clearly indicated that the main impact of helix F deletion is an increase in Trp-305 flexibility and solvent accessibility. This modification likely facilitated membrane insertion of this Trp in DelF.

We therefore postulated the following scenario for PE membrane insertion. In PE, the low pH sensor that prevents Trp-305 exposure under neutral pH conditions would be Glu-359 and/or Asp-358 residues that H-bond Trp-305 and N-cap helix F, respectively (Fig. 1A). Because helix F is made of 5 residues only, most amide protons are not involved in standard (i,i+4) α-helical H-bonding, and the H-bonding of the amide proton of Gly-361 with the side chain of Asp-358 is likely essential. Because the negative charge of Asp-358 is largely involved in

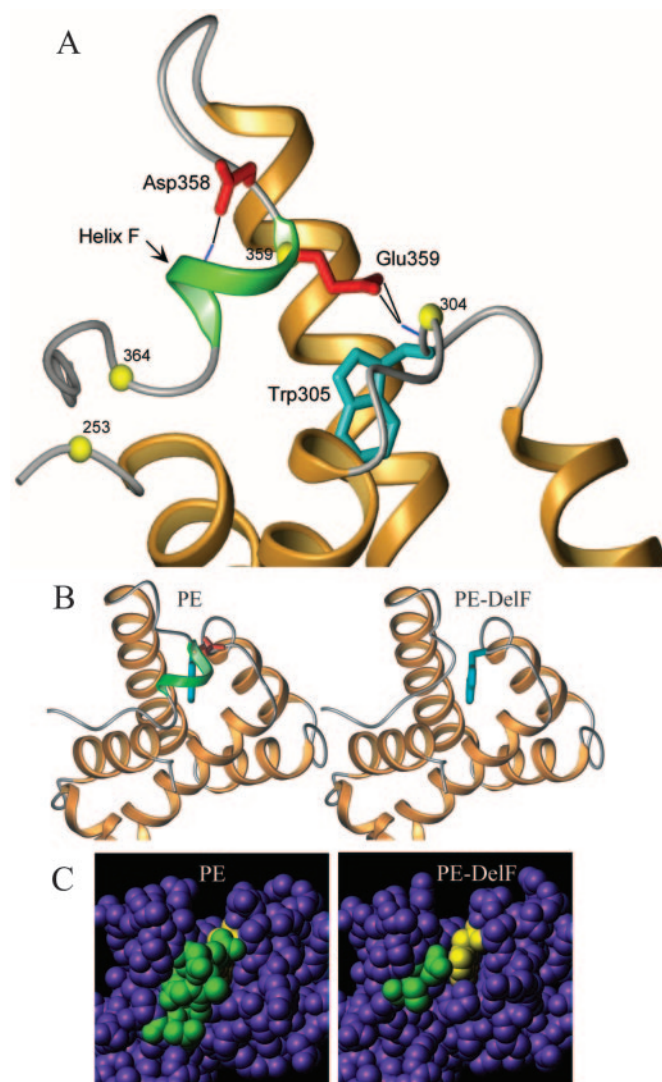


FIG. 1. Representation of the studied portion of the PE translocation domain. A, ribbon representation. Helices are shown in brown, except the helix F, which is shown in green. Side chains of Trp-305 (cyan), Asp-358 and Glu-359 (red) are shown as sticks. The NH bonds of residues 305 and 361 are displayed as blue lines and their H-bonds with Asp-358 and Glu-359 as black lines. Ca atoms of residues that were mutated into cysteines in the S304C,E359C (PE-SL) and G253C,N364C (PE-LL) mutants are shown as yellow spheres. B, comparison of wild-type PE and the DelF mutant. The removal of helix F (green ribbon) in PE, including Glu-359 (red sticks, left image), widely opens access of Trp-305 to the solvent in the DelF mutant (cyan sticks). C, same as panel B but using Corey-Pauling-Koltun. Helix F is in green, Trp-305 in yellow, and the rest of the molecule is in purple.

the N-capping stabilizing effect (22), its neutralization by lowering the pH would significantly destabilize helix F, in turn triggering Trp-305 side chain exposure, finally leading to insertion into the endosome membrane. This insertion would be a prerequisite for translocation. In this report, we have presented data that validate this model.

Mutant Description—Mutating Trp-305 into Phe or Ala decreased PE toxicity by 3- or 13-fold, respectively. These mutants were specifically affected in their translocation activity. Hence, PE-W305F and PE-W305A translocated 30 and 55% less actively than PE, respectively (data not shown). These results demonstrated that Trp-305 is involved in PE translocation activity.

Nevertheless, because Trp-305 mutants lack a Trp it was not possible to examine the PE insertion process using a comparative tryptophan fluorescence study of these mutants. More-

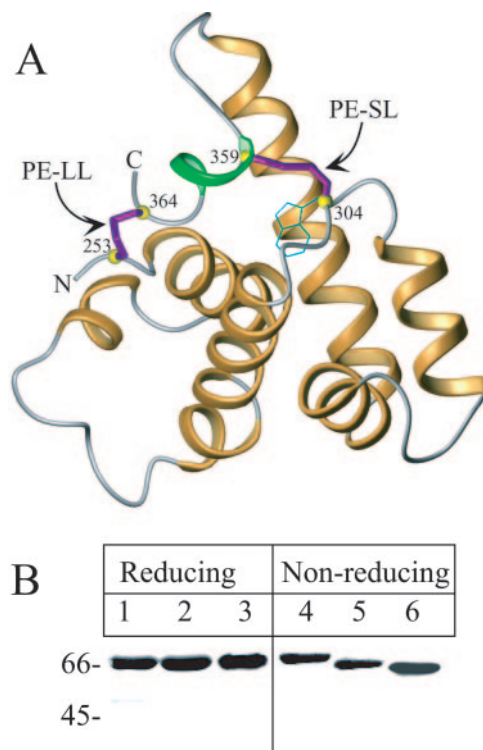
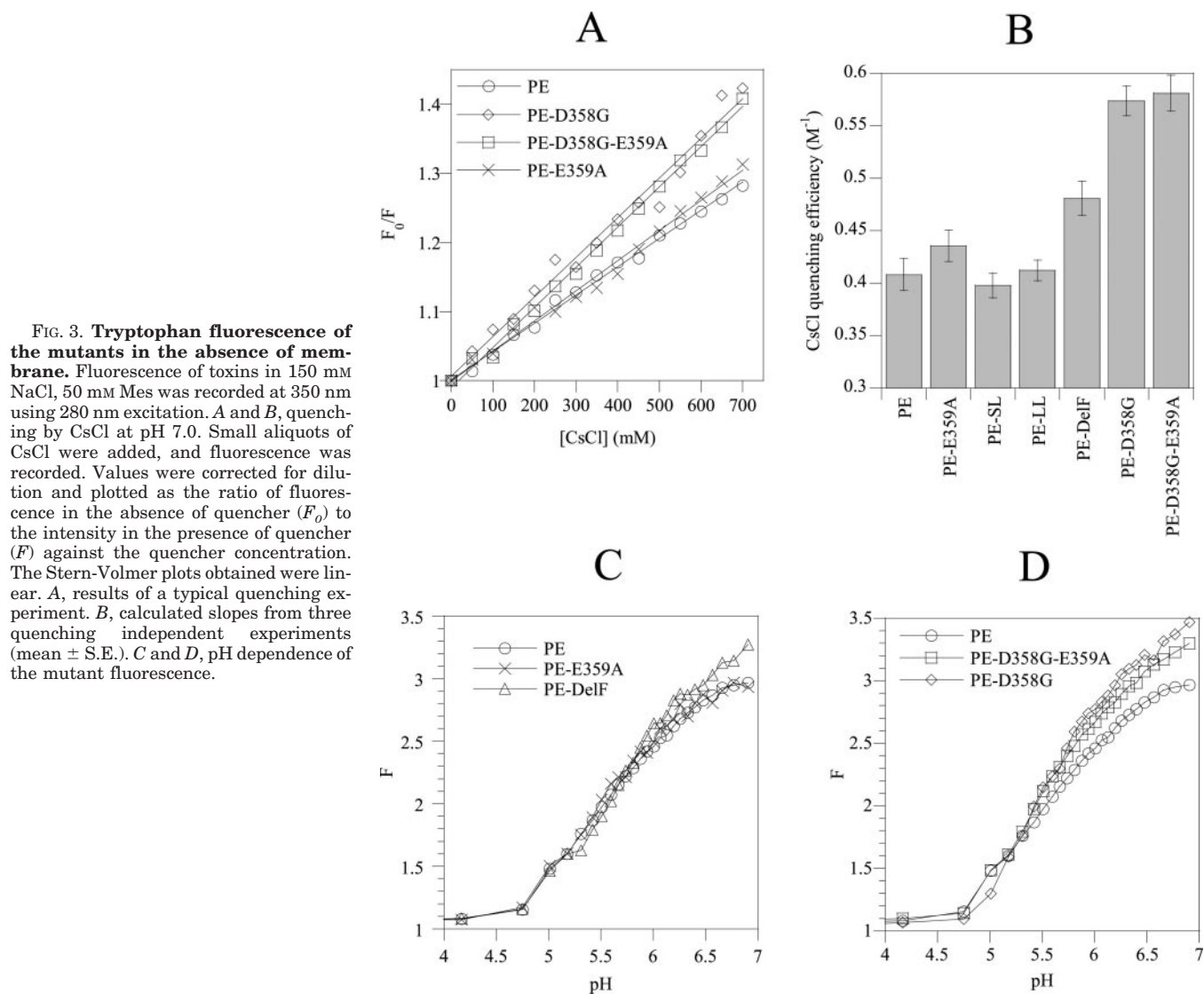


FIG. 2. Characterization of mutants bearing an additional disulfide. A, modeling of PE-SL (PE-S304C,E359C) and PE-LL (PE-G253C,N364C). The two mutants were modeled separately, but because no significant structural deviation was introduced by the disulfide bridges, both disulfide bridges (yellow spheres and purple sticks) are displayed on the same structure. B, SDS-PAGE analysis of purified toxins. Proteins were separated on 10% acrylamide gels under reducing or non-reducing conditions as indicated before gel staining with Coomassie blue. Lanes 1 and 4, PE; lanes 2 and 5, PE-SL; lanes 3 and 6, PE-LL. Molecular mass is shown (kDa).

over, Trp-305 participates in the hydrophobic core of the molecule. This raises the possibility that the effect of the Trp-305 mutation on PE translocation and toxicity could be indirect, through structure modifications. We therefore prepared for this study mutants that still own Trp-305; to assess whether the side chain of Trp-305 might be involved in membrane interactions, we locked it within its hydrophobic pocket. To this end, we replaced the hydrogen bonding between the Trp-305 backbone and Glu-359 side chain by a disulfide bridge generated by mutating residues 304 and 359 to Cys (Fig. 2A). This PE-304C, 359C, termed PE-SL (for small loop), was used throughout this study as a negative control for membrane insertion.

We also prepared a PE with a control disulfide bridge in another part of the molecule. This mutant, PE-253C,364C, termed PE-LL (for large loop), possesses an additional disulfide that links the amino and carboxyl termini of domain II (Fig. 2A). The structural analysis showed that both disulfide bridges could form with minimal modification of the protein structure. This formation was monitored by free thiol determination (not shown) and SDS-PAGE analysis. Additional disulfides generally enhance electrophoretic mobility (23); this was the case for both PE-SL and PE-LL under non-reducing conditions, although they migrate at the PE level after disulfide reduction (Fig. 2B). Hence, the introduced Cys generated the expected disulfide. Other mutants were made on Asp-358 and Glu-359 as indicated. We checked that the mutant conformation, endocytosis, furin-mediated processing, intracellular routing, and catalytic activity were not altered (see “Materials and Methods”).

F Helix Destabilization Leads to Increased Trp-305 Accessibility at Neutral pH—We first assessed whether helix F desta-



bilization would actually result in increased Trp-305 accessibility. To this end, we used Trp fluorescence quenching by cesium ions (24). Although PE has 11 Trp, it proved possible to monitor Trp-305 exposure using the entire molecule. Indeed, fluorescence of DelF, and especially of the D358G and D358G,E359A mutants, was up to 50% more sensitive to quenching by Cs^+ than PE and mutants with an intact helix F such as E359A (Fig. 3, *A* and *B*). Hence, mutants in which helix F was absent (DelF) or destabilized (D358G or D358G,E359A) exposed a tryptophan residue, most likely Trp-305, that is normally buried inside the wild-type toxin.

Differences in tryptophan exposure among the mutants were also observed using direct fluorescence measurements and were pH dependent (Fig. 3, *C* and *D*). At neutral pH, DelF, D358G, and D358G,E359A showed higher intrinsic fluorescence compared with PE or the E359A mutant. This difference, likely due to the relief of internal quenching, was maximum at pH 7.0 and reached 17% for the most affected mutant (D358G). The gap with PE gradually decreased upon acidification, and all curves were superimposed at pH <5.5.

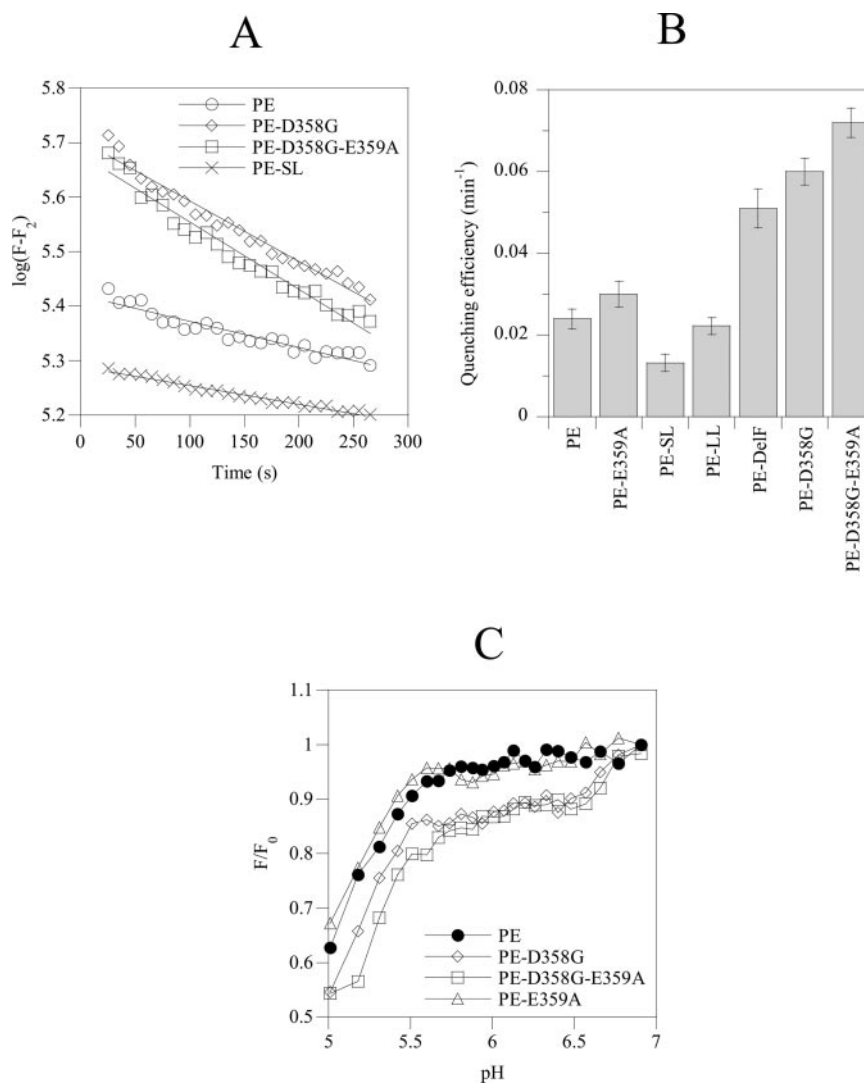
The E359A results indicate that hydrogen binding of Glu-359 with Trp-305 is not essential for restricting solvent accessibility of Trp-305. In contrast, deletion of helix F significantly increased solvent accessibility of Trp-305 at neutral pH, in agreement with DelF molecular modeling. As expected, the D358G mutation yielded results similar to DelF, showing that

removal of the helix F N-cap strongly destabilized this helix. These data also suggest that, upon acidification, Trp-305 is gradually exposed to the solvent in native PE.

Trp-305 Is a Key Residue Allowing PE Membrane Insertion—To assess the role of Trp-305 in membrane insertion, we monitored the ability of the different mutants to insert into model membranes at acidic pH (pH 5.5). To this end, we used SUVs containing brominated phospholipids that enabled us to quench Trp fluorescence of any membrane-inserted PE (7). Insertion efficiencies were monitored using the slope of the quenching curve. Consistent with previous findings (7), at pH 5.5 PE efficiently inserted within SUVs (Fig. 4, *A* and *B*). Mutants in which helix F was destabilized inserted \sim 2-fold (DelF), \sim 2.5-fold (D358G), and \sim 3-fold (D358G,E359A) more quickly than PE. PE-SL inserted \sim 2-fold less efficiently than PE into SUVs, whereas the control disulfide in PE-LL had no significant effect on insertion. Hence, introduction of a 304–359 disulfide in PE specifically inhibited membrane penetration, most likely by preventing membrane insertion of Trp-305. Throughout this study, the PE-E359A mutant behaved just like PE, indicating that the PE-D358G and PE-SL phenotypes do not merely result from charge modification.

Mutants favoring access of Trp-305 to the outside thus inserted more actively into membranes, whereas locking the Trp-305 side chain into its hydrophobic cavity inhibited insertion. Altogether, these data strongly suggest that Trp-305 exposure

FIG. 4. Ability of the different mutants to insert into model membranes as monitored using fluorescence quenching. Brominated SUVs were added to a solution of toxin at pH 5.5. Fluorescence quenching kinetics can be described with a two-stage model involving a bi-exponential function: $F = F_1 e^{-at} + F_2 e^{-bt}$. **A**, the first exponential process of the kinetics was plotted as the $\log(F - F_2)$ against time. The plots obtained were linear. **B**, slope values ($n =$ four experiments). **C**, pH dependence of mutant insertion into brominated SUVs. Fluorescence was measured at the indicated pH in the presence or absence of brominated SUVs. The results ($n = 3$, error bars fell within the symbol size) show the values of fluorescence with quencher (F) relative to that without quencher (F_0). PE-E359P was not tested in this insertion assay.



is a prerequisite for low pH-induced PE insertion into model membranes and that the Trp-305 side chain is the PE initial membrane anchor.

Asp-358 Is the Low pH Sensor Triggering Trp-305 Exposure and PE Membrane Insertion—Because PE penetrates into membranes upon acidification to pH 5.0–5.5 (7), Trp-305 insertion should be tightly regulated by pH. In several toxins, such as botulinum toxins, diphtheria toxin, and colicins whose conformation changes in response to low pH, acidic residues were identified as low pH sensors triggering structural modifications (25–27). We therefore monitored the pH dependence of membrane insertion for all Asp-358/Glu-359 mutants using Trp fluorescence quenching by brominated liposomes. In agreement with previous studies (7), PE significantly inserted into brominated SUVs only below pH 5.7–5.5 (Fig. 4C). Nevertheless, mutants in which Asp-358 was replaced by Gly (D358G and D358G,E359A) started inserting themselves into SUVs as soon as the pH dropped to 6.8. At pH 6.6, for these mutants 20–25% of the molecules inserted relative to the maximum insertion, which was observed at pH 5.0.

Hence, a low pH sensor was almost entirely lost upon the D358G mutation, which enabled significant insertion at pH <6.8 instead of pH <5.7. These values are within the pH range of the endocytic pathway (28), and this ~1.1-pH unit difference will have strong biological implications (see below). We concluded that Asp-358 is the low pH sensor that triggers helix F

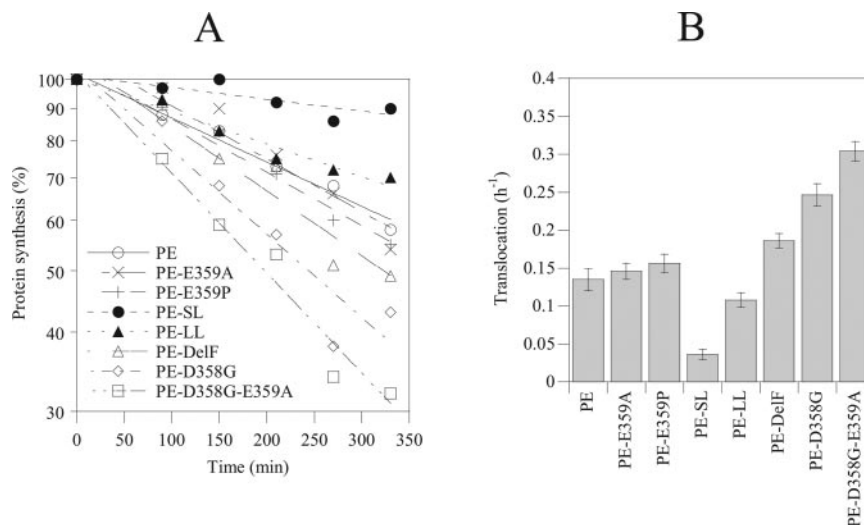
collapse at acidic pH, thereby enabling the Trp-305 exposure required to initiate PE membrane insertion.

Trp-305 Exposure Directly Regulates Membrane Translocation—It was tempting to speculate that, compared with PE, any mutant inserting into membranes at less acidic pH would translocate more efficiently to the cytosol during cell intoxication, especially if intoxication significantly results from direct translocation of the entire toxin through the endosome membrane (6). Indeed, endosome acidity is established by the vacuolar ATPase that gradually lowers the pH in the organelle lumen (29), and such mutants should therefore be able to translocate earlier to the cytosol. We examined mutant membrane translocation by monitoring kinetics of protein synthesis inhibition. Translocation is the rate-limiting step for cell killing by PE, and protein synthesis inactivation curves plotted as $\log(\text{rate protein synthesis})$ versus time directly reflect translocation efficiency (30, 31).

The translocation efficacy of PE-SL (which bears the additional disulfide preventing Trp-305 exposure) was only 25% of that of native PE (Fig. 5), whereas the control disulfide present in PE-LL weakly inhibited (by 20%) translocation. Hence, Trp-305 exposure is required for PE insertion and translocation.

Mutants of Glu-359 (E359P and E359A) were not affected in their translocation efficiency, whereas helix F disruption by deletion or N-capping suppression enhanced the translocation efficacy by 40% (Delf), 85% (D358G), or 125% (D358G,E359A).

FIG. 5. Translocation activity of the mutants. Translocation efficacy was measured by monitoring the kinetics of protein synthesis inactivation. L929 cells were treated with 10 μ M toxin before assaying protein synthesis for 1 h using [35 S]methionine. Cells were then lysed and proteins harvested for scintillation counting. *A*, the protein synthetic rate of intoxicated cultures is plotted as percentage of non-intoxicated cultures versus the midpoint of [35 S]methionine pulse. *B*, translocation activity was calculated from the slope of the cell-killing curve. It is expressed as the inverse of t_{50} , which is the time required for 10 μ M toxin to inhibit protein synthesis by 50%.



Similar data (not shown) were obtained using a cell-free translocation assay based on the use of lymphocyte endosomes loaded with PE (6, 15).

Enhancing Trp-305 Exposure Increases Toxicity—Because translocation is thought to be the rate-limiting step for cell intoxication by PE (30) and because some mutants translocated more efficiently than PE, one might expect these mutants to be more toxic than PE. This was indeed the case (Fig. 6A). Mutations on Glu-359 affected toxicity either poorly (PE-359P) or not at all (PE-359A), whereas PE-DelF, PE-358G, and PE-358G,359A were 3-, 6-, and 7-fold more toxic than PE, respectively. Hence, PE-358G,359A is the most toxic PE mutant ever obtained. Regarding PE with inserted disulfides, PE-SL was the least toxic molecule (~4-fold less toxic than PE), whereas PE-LL cytotoxicity was similar to that of PE. Nevertheless, during this assay, which requires 48-h contact with cells, and because the introduced disulfides are exposed at the surface of the protein, they might have been prematurely reduced, *i.e.* before the insertion or translocation step of the intoxication procedure. Hence, toxicity differences between PE-SL/PE-LL and PE are likely more pronounced than those measured in this assay.

Mutants that inserted more efficiently into model membranes (DelF, D358G, D358G,E359A) were those that translocated the most efficiently; conversely, PE-SL inserted and translocated very poorly. Altogether, our data showed a strict and significant linear relationship between insertion and translocation (Fig. 6B) but also between translocation and toxicity (Fig. 6C). Hence, all of these PE properties are tightly linked.

DISCUSSION

Because the PE structure is devoid of hydrophobic helices that are commonly used by bacterial toxins such as diphtheria toxin, colicins, or botulinum toxins to anchor into membranes upon acidification (9, 25), no model or information was available on the PE membrane insertion mechanism. The PE membrane insertion system identified here consists of two separate units, a membrane anchor (Trp-305 side chain) and a pH-dependent device hiding this anchor at neutral pH and unmasking it at low pH. The helix F of the translocation domain is the structure that masks Trp-305 and collapses at acidic pH. Its N-capping residue, Asp-358, is the pH sensor that destabilizes the helix F at low pH.

This membrane insertion system is original in two ways, first because anchoring by a single Trp is sufficient to trigger PE insertion and translocation and, second, because a single acidic

residue is enough to control low pH-mediated insertion. Acidic residues are very efficient for N-capping, and ~40% of their stabilization energy is provided by their negative charge (22). It is probably because helix F is so short, thus precluding cooperative H-bonding stabilization, that acidification leading to neutralization of the charge of Asp-358 was sufficient to trigger helix F collapse. This conclusion was further confirmed using the AGADIR program (32) to predict peptide helical content, because the Asp to Gly mutation was predicted to destabilize helix F.

The D358G and D358G,E359A mutants on one side and PE and E359A on the other side clearly behaved differently in membrane insertion, translocation, and toxicity assays, ruling out a significant role for Glu-359 in controlling insertion. Hence, Asp-358 is the pH sensor triggering helix F destabilization, and Glu-359, although H-bonding to the Trp-305 backbone, does not play a significant role in this process. Nevertheless, in all assays involving membranes, the D358G,E359A mutant was slightly but consistently more efficient than D358G. We concluded that, although it has no effect on its own, the E359A mutation slightly enhances the destabilizing effect of the D358G mutation.

Although acidic residues are often considered as low pH sensors inducing or participating in conformational changes within the translocation domain of low pH-activated toxins such as botulinum toxins (25) and diphtheria toxin (26), the exact role of specific acidic residues has only been identified for colicins. In that case, 3 Asp residues distributed within two helices triggered disruption of the helical structure upon acidification (27). Hence, acidic residues are used by several toxins as low pH sensors to induce a destabilizing effect on specific target and key helices whose collapse will enable structural rearrangements upon low pH exposure. These acidic residues (Asp until now) can control the integrity of these helices because they belong to the helix residues (27) or because they are the N-cap residue (this study).

The poor ability of PE-SL to insert into model membranes (Fig. 4) clearly indicated that Trp-305 side chain exposure is required to initiate this process. Nevertheless, other structural elements are likely implicated at a later stage in the insertion mechanism. The other tryptophan of the translocation domain, *i.e.* Trp-281, which is required for toxicity (33) and only partially exposed to the solvent in the three-dimensional structure at neutral pH (12), might play a role at that time.

The strong correlation between mutant translocation activity and toxicity (Fig. 6C) confirmed that translocation is a step

FIG. 6. Mutant toxicity. L929 cells were treated for 24 h with the indicated toxin concentration before adding [35 S]methionine. After another 24 h, cells were lysed and proteins harvested for scintillation counting. *A*, mutant toxicity is expressed as the IC_{50} that is the toxin concentration resulting in 50% protein synthesis inhibition. *B*, correlations between membrane insertion (efficiency of quenching by brominated SUVs) and translocation ($1/t_{50}$). *C*, correlation between translocation ($1/t_{50}$) and toxicity (IC_{50}).

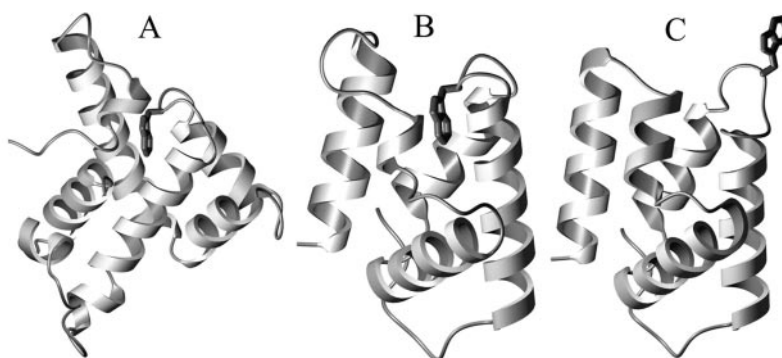
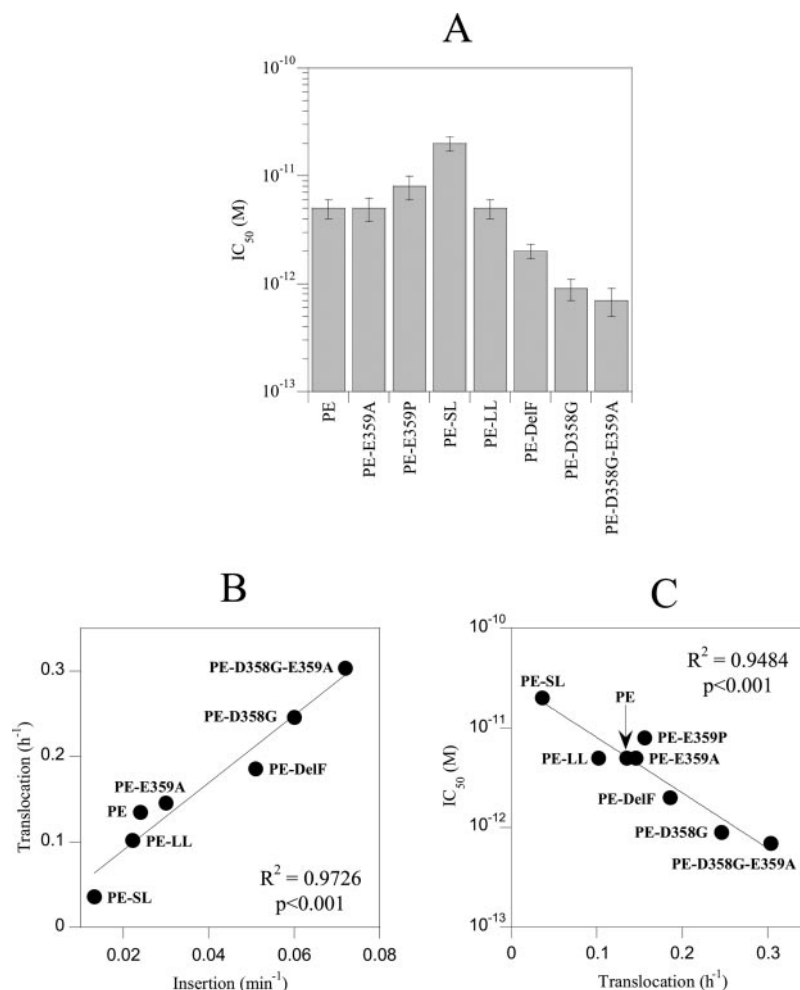


FIG. 7. Comparison of the environment of Trp-305 in domain II of PE with that of Trp-187 in domain III of human annexin-V. In both cases, PE (*A*) and annexin-V (*B*) (Protein Data Bank accession code 1anw), the tryptophan lies at the tip of a loop between consecutive helices and is buried within the core of an all- α domain. The short helix D in annexin-V occupies, with respect to the tryptophan, a position quite similar to the position of helix F in PE. *C*, conformation of human annexin-V at high calcium concentration (Protein Data Bank accession code 1anx). The tryptophan is expelled from the protein core, and helix D is significantly rearranged.

that limits PE toxicity (15, 30). This direct translocation/toxicity link contrasts with the processing/toxicity relationship. Processing is the first step of a model implicating the endoplasmic reticulum in the process of cell intoxication by PE. Upon exposure to low endosomal pH, some PE molecules (5–10%) are cleaved by furin between Arg-279 and -280 to generate a 37-kDa carboxyl-terminal fragment containing most of domain II and the entire domain III (1, 34). The last 5 residues of the toxin (REDLK) are required for toxicity (35). The carboxyl-terminal lysine is thought to be removed at an early stage of the intoxication process, presumably by plasma carboxyl pep-

tidase(s) (34). This would allow the 37-kDa fragment to bind to the KDEL receptor within the *trans*-Golgi network, triggering its retrograde transport to the endoplasmic reticulum for translocation to the cytosol, possibly through Sec61 channels (1, 34). Several studies showed that there is no clear correlation between processing and toxicity. Indeed, mutants more efficiently processed by furin intracellularly were found to be consistently less toxic than PE (33, 36). Our mutants also showed a lack of correlation between processing and toxicity because, within cells, they were cleaved by furin with the same efficiency as native PE (data not shown) although their toxicity varied over

a 1–30 scale (Fig. 6A). Hence, our data are consistent with a model involving not PE processing (1) but direct transport of the entire toxin through the endosome membrane (6, 8). Both models might be valid. Indeed, we have evidence that both processed and entire PE molecules are involved in cell intoxication.²

PE is the first prokaryotic protein whose membrane insertion relies on a Trp residue. Nevertheless, a similar process has been documented for annexin-V, an eukaryotic protein that binds to membranes in a calcium-dependent manner. Human annexin-V contains a single Trp that is buried within domain III in the absence of calcium (Fig. 7B). The addition of calcium induces a local conformational change that causes the formation of a calcium binding site in domain III and brings the tryptophan onto the surface of the protein (Fig. 7C), a modification that is largely involved in membrane binding. Indeed, mutating this Trp to Ala specifically decreased the efficiency of Ca²⁺-triggered membrane insertion of annexin-V by 50% (37). Despite the difference in the stimulus leading to a surface-exposed Trp in PE (acidification) and annexin-V (calcium), the topologies around the Trp appear to be strikingly similar (Fig. 7, A and B). In both cases, the Trp is located at the tip of a loop between two helices and is entirely buried inside an all-helical domain. Helix D in annexin-V domain III is topologically equivalent to helix F in the PE translocation domain. Moreover, these helices are the shortest of their respective domains. Hence, the structural organization of both domains is such that a minute destabilization restricted to these small helices, *i.e.* of helix D for annexin-V (38) or helix F for PE (this study), allows the Trp to move from the interior to the surface of the molecule without requiring extensive domain unfolding. Because a similar buried/exposed Trp structural switch seems to occur in these two unrelated proteins, this could be a general process that might function in other proteins as well when regulated membrane insertion has to be achieved.

Our study has elucidated a molecular device that triggers acid-induced PE membrane insertion. We also obtained the most toxic PE mutant ever produced so far (PE-358G, 359A, which is ~7-fold more toxic than PE). Designing more potent toxins should enable easier clinical uses of immunotoxins (2, 39). This mutant could therefore be used to prepare more active PE-based immunotoxins.

Acknowledgment—We thank Claude Roustan for advice on fluorescence spectroscopy.

² J. Morlon-Guyot, J. Méré, A. Bonhoure, and B. Beaumelle, manuscript in preparation.

REFERENCES

- Pastan, I., Chaudhary, V., and FitzGerald, D. (1992) *Ann. Rev. Biochem.* **61**, 331–354
- Reiter, Y., and Pastan, I. (1998) *Trends Biotechnol.* **16**, 513–520
- Allured, V. S., Collier, R. J., Carroll, S., and McKay, D. B. (1986) *Proc. Natl. Acad. Sci. U. S. A.* **83**, 1320–1324
- Hwang, J., FitzGerald, D. J., Adhya, S., and Pastan, I. (1987) *Cell* **48**, 129–136
- Kounnas, M. Z., Morris, R. E., Thompson, M. R., FitzGerald, D. J., Strickland, D. K., and Sealinger, C. B. (1992) *J. Biol. Chem.* **267**, 12420–12423
- Alami, M., Taupiac, M. P., Reggio, H., Bienvenue, A., and Beaumelle, B. (1998) *Mol. Biol. Cell* **9**, 387–402
- Jiang, J. X., and London, E. (1990) *J. Biol. Chem.* **265**, 8636–8641
- Rasper, D. M., and Merrill, A. R. (1994) *Biochemistry* **33**, 12981–12989
- Parker, M. W., and Pattus, F. (1993) *Trends Biochem. Sci.* **18**, 391–395
- Altschul, S. F., Gish, W., Miller, W., Myers, E. W., and Lipman, D. J. (1990) *J. Mol. Biol.* **215**, 403–410
- Holm, L., and Sander, C. (1996) *Science* **273**, 595–603
- Wedekind, J. E., Trame, C. B., Dorywalska, M., Koehl, P., Raschke, T. M., McKee, M., FitzGerald, D., Collier, R. J., and McKay, D. B. (2001) *J. Mol. Biol.* **314**, 823–837
- Kasturi, S., Kihara, A., FitzGerald, D. J., and Pastan, I. (1992) *J. Biol. Chem.* **267**, 23427–23433
- Jinno, Y., Ogata, M., Chaudhary, V. K., Willingham, M. C., Adhya, S., FitzGerald, D., and Pastan, I. (1989) *J. Biol. Chem.* **264**, 15953–15959
- Taupiac, M. P., Bebién, M., Alami, M., and Beaumelle, B. (1999) *Mol. Microbiol.* **31**, 1385–1393
- Sali, A., and Blundell, T. L. (1993) *J. Mol. Biol.* **234**, 779–815
- Koradi, R., Billeter, M., and Wuthrich, K. (1996) *J. Mol. Graph.* **14**, 51–54, 29–32
- Landt, O., Grunert, H.-P., and Hahn, U. (1990) *Gene* **96**, 125–128
- Vouilhoux, R., Taupiac, M. P., Czjzek, M., Beaumelle, B., and Filloux, A. (2000) *J. Bacteriol.* **182**, 4051–4058
- Morlon-Guyot, J., Helmy, M., Lombard-Frasca, S., Pignol, D., Pieroni, G., and Beaumelle, B. (2003) *J. Biol. Chem.* **278**, 17006–17011
- Vendeville, A., Rayne, F., Bonhoure, A., Bettache, N., Montcourrier, P., and Beaumelle, B. (2004) *Mol. Biol. Cell* **15**, 2347–2360
- Serrano, L., and Fersht, A. R. (1989) *Nature* **342**, 296–299
- Eppens, E. F., Nouwen, N., and Tommassen, J. (1997) *EMBO J.* **16**, 4295–4301
- Eftink, M. R., and Ghiron, C. A. (1981) *Anal. Biochem.* **114**, 199–227
- Lacy, D. B., and Stevens, R. C. (1999) *J. Mol. Biol.* **291**, 1091–1104
- Ren, J., Sharpe, J. C., Collier, R. J., and London, E. (1999) *Biochemistry* **38**, 976–984
- Musse, A. A., and Merrill, A. R. (2003) *J. Biol. Chem.* **278**, 24491–24499
- Gruenberg, J., and Maxfield, F. R. (1995) *Curr. Opin. Cell Biol.* **7**, 552–563
- Clague, M. J., Urbe, S., Aniento, F., and Gruenberg, J. (1994) *J. Biol. Chem.* **269**, 21–24
- Hudson, T. H., and Neville, D. M., Jr. (1987) *J. Biol. Chem.* **262**, 16484–16494
- Youle, R. J., and Neville, D. M., Jr. (1982) *J. Biol. Chem.* **257**, 1598–1601
- Muñoz, V., and Serrano, L. (1994) *Nat. Struct. Biol.* **1**, 399–409
- Zdanovskiy, A. G., Chiron, M., Pastan, I., and FitzGerald, D. J. (1993) *J. Biol. Chem.* **268**, 21791–21799
- Hessler, J. L., and Kreitman, R. J. (1997) *Biochemistry* **36**, 14577–14582
- Chaudhary, V. K., Jinno, Y., FitzGerald, D. J., and Pastan, I. (1990) *Proc. Natl. Acad. Sci. U. S. A.* **87**, 308–312
- Chiron, M. F., Ogata, M., and FitzGerald, D. (1996) *Mol. Microbiol.* **22**, 769–778
- Campos, B., Mo, Y. D., Mealy, T. R., Li, C. W., Swairjo, M. A., Balch, C., Head, J. F., Retzinger, G., Dedman, J. R., and Seaton, B. A. (1998) *Biochemistry* **37**, 8004–8010
- Sopkova-De Oliveira Santos, J., Fischer, S., Guilbert, C., Lewit-Bentley, A., and Smith, J. C. (2000) *Biochemistry* **39**, 14065–14074
- Kreitman, R. J. (1999) *Curr. Opin. Immunol.* **11**, 570–578